Check for updates

Childbirth Computational Models: Characteristics and Applications

Sheng Chen
Departments of Mechanical and Biomedical Engineering,
Michigan State University,
428 S. Shaw Lane,
East Lansing, MI 48824
e-mail: chensh38@msu.edu

Michele J. Grimm[1]
Mem. ASME
Departments of Mechanical and Biomedical Engineering,
Michigan State University,
428 S. Shaw Lane,
East Lansing, MI 48824
e-mail: mgrimm@msu.edu

The biomechanical process of childbirth is necessary to usher in new lives—but it can also result in trauma. This physically intense process can put both the mother and the child at risk of injuries and complications that have life-long impact. Computational models, as a powerful tool to simulate and explore complex phenomena, have been used to improve our understanding of childbirth processes and related injuries since the 1990s. The goal of this paper is to review and summarize the breadth and current state of the computational models of childbirth in the literature—focusing on those that investigate the mechanical process and effects. We first summarize the state of critical characteristics that have been included in computational models of childbirth (i.e., maternal anatomy, fetal anatomy, cardinal movements, and maternal soft tissue mechanical behavior). We then delve into the findings of the past studies of birth processes and mechanical injuries in an effort to bridge the gap between the theoretical, numerical assessment and the empirical, clinical observations and practices. These findings are from applications of childbirth computational models in four areas: (1) the process of childbirth itself, (2) maternal injuries, (3) fetal injuries, and (4) protective measures employed by clinicians during delivery. Finally, we identify some of the challenges that computational models still face and suggest future directions through which more biofidelic simulations of childbirth might be achieved, with the goal that advancing models may provide more efficient and accurate, patient-specific assessment to support future clinical decision-making. [DOI: 10.1115/1.4049226]

Keywords: childbirth, computational models, childbirth injuries, childbirth characteristics

1 Introduction

Parturition—or childbirth—is a complex mechanical process that includes a risk of injury to both the mother and infant. Many of these injuries are mechanical in nature—resulting from stresses and strains that are experienced by the tissues and anatomical structures of the mother and child during labor and delivery. In the infant, these injuries most commonly include bony fractures, small vessel hemorrhages, hematomas, and nerve injuries in the infant [1], while for the mother the most common mechanical injury is damage to the pelvic floor and/or perineum [2].

For many years, clinical researchers have focused efforts on understanding the mechanism of childbirth, identifying risk factors for childbirth-related injuries, and exploring management protocols to support and assist a difficult labor. Different approaches have been utilized to achieve those research goals.

Statistical analysis of retrospective observational data is one approach. By looking into data that describe a broad range of births, correlation coefficients between a difficult labor scenario and specific maternal/fetal parameters can be achieved. This can help to identify risk factors for a difficult labor or delivery-associated morbidities. Retrospective observational data have the advantage of revealing correlations between characteristics of the mother and/or baby and birth-related outcomes, but they do not reveal the mechanism of injury, and—in many cases—struggle to identify causative factors for injuries. For example, retrospective observational data have identified that risk factors for neonatal brachial plexus palsy (NBPP) include fetal malposition, labor induction, labor abnormalities, operative vaginal delivery, fetal macrosomia, and shoulder dystocia (i.e., a delay in delivery of the shoulders), among which, shoulder dystocia is the only factor that is statistically significant for the occurrence of NBPP [3]. Nonetheless, shoulder dystocia alone cannot be used to predict the occurrence of NBPP, since even with strong associations between a risk factor (e.g., shoulder dystocia) and a given outcome (e.g., NBPP), the use of relative risk or odds ratios can lead to prediction of large numbers of false positive cases (e.g., shoulder dystocia without NBPP) [3].

Physical birth simulators provide another approach to understand the birth process. Birth simulators can offer clinicians hands-on experience during training to practice interventions associated with delivery-related emergencies. Studies have shown that use of birth simulators in clinician training contributes to better management of different labor scenarios [4–6]. However, physical birth models suffer a few disadvantages in terms of offering deeper insights into mechanisms of injuries related to the birth process. First, these physical models have limited capability to represent patient-specific information. They are usually made to simulate a generic childbirth situation (i.e., average sized mother and fetus). Once constructed, it is hard to adapt a simulator to patient-specific measurements. Second, physical childbirth models have limited complexity in terms of representing all elements that are crucial to the mechanics of the birth process. Soft tissue geometry (e.g., pelvic floor muscles) is mostly oversimplified in physical childbirth models, with no attempt made at validating soft tissue mechanical properties [7–10]. For complicated physiological processes (e.g., uterine contractions and maternal pushing), it becomes impractical to accurately simulate these on a physical model.

Childbirth computational models can overcome some of the limitations that physical childbirth models have and offer deeper insights into the mechanisms of fetal and maternal injury associated with the birth process. Through in vivo imaging techniques (e.g., MRI, CT, and ultrasound), childbirth computational models

[1]Corresponding author.
Manuscript received September 1, 2020; final manuscript received November 24, 2020; published online February 19, 2021. Assoc. Editor: Raffaella De Vita.

 Copyright © 2021 by ASME

Downloaded from http://asmedigitalcollection.asme.org/biomechanical/article-pdf/143/5/050801/6641401/bio_143_05_050801.pdf by Michigan State University user on 11 March 2021

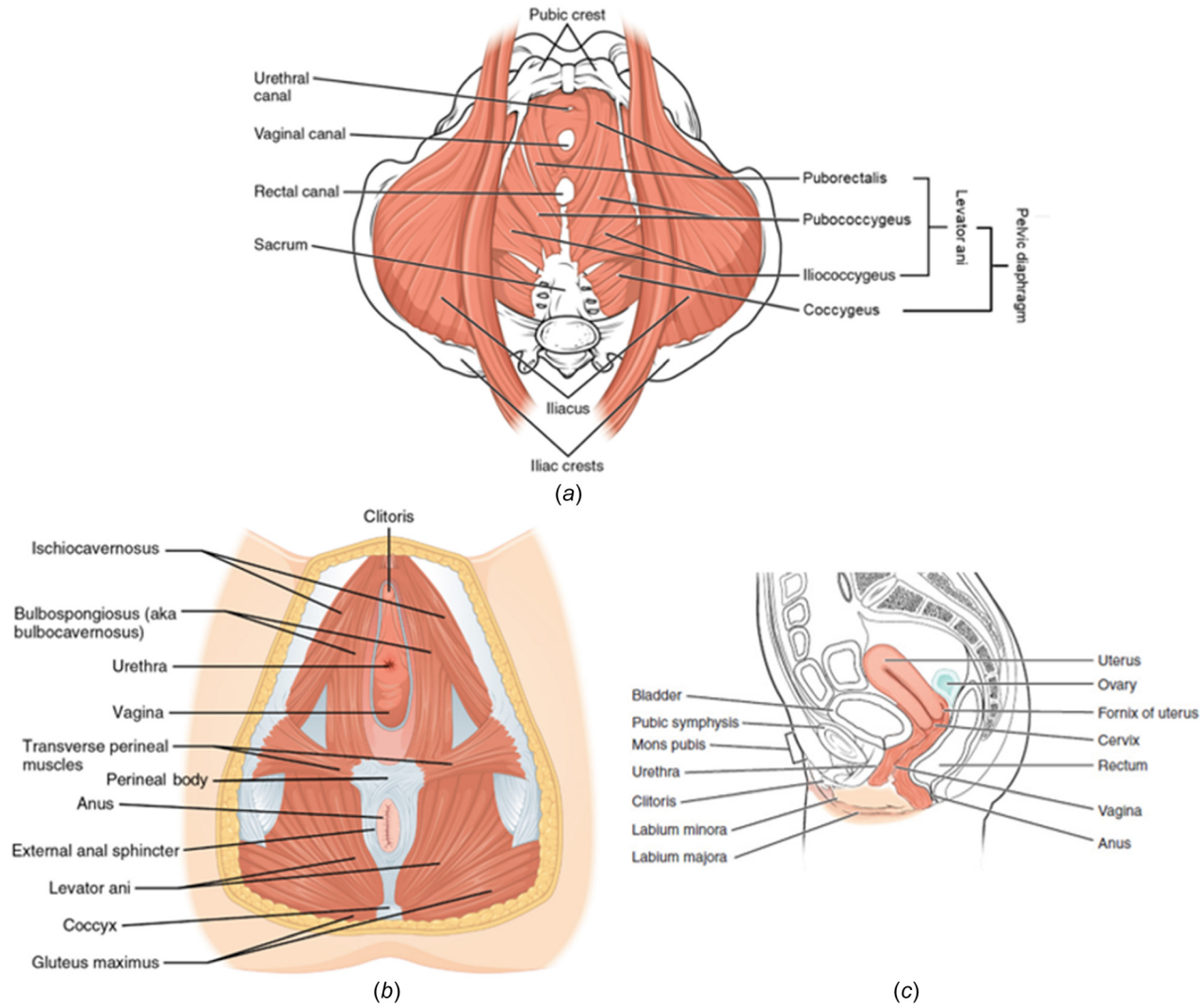

Fig. 1 Illustration of maternal anatomy related to childbirth. (*a*) pelvic floor, (*b*) perineum, (*c*) reproductive and urinary systems. Reprinted with permission from *OpenStax*.[2] Annotations are slightly modified by the authors of this review paper compared to the original figures in *OpenStax*.

can include patient-specific, three-dimensional (3D) geometries of bony structures, soft tissues, the fetus, etc. Accurate mechanical properties (e.g., anisotropy, nonlinearity, and viscoelasticity) of biological soft tissues can be included by applying proper constitutive models with parameters that match in vivo experimental data. Critical physiological processes during childbirth, like uterine contractions and maternal pushing, can also be included in a numerical model. Researchers have been building numerical models to study the effect of the birth process on maternal and infant tissues since the 1990s. With the advancement of computer hardware and numerical modeling software, childbirth computational models have become more realistic and capable of exploring more complex topics. This review examines the current state of computational modeling of childbirth, with a focus on the various approaches that have been used for the model characteristics as well as the range of applications these models can be used for. It includes an identification of challenges associated with computational modeling of the birth process as well as a discussion of some possible future directions.

[2]https://openstax.org/details/books/anatomy-and-physiology

2 Model Characteristics

2.1 Maternal Anatomy. Proper imaging techniques are necessary to obtain accurate geometry for maternal structures, including the pelvic floor, the perineum, and the urinary and reproductive systems (Fig. 1). MRI (magnetic resonance imaging) is the dominant imaging technique that has been used to develop the anatomical parameters for computational birth models [11–28], followed by CT (computed tomography) [15,16,22,23,29,30]. These techniques can be used to determine normal ranges of anatomical parameters and to develop patient-specific models.

Both pregnant and nonpregnant women have been included as subjects for imaging to determine the arrangement and size of anatomical structures. Nonpregnant women may be included because of the challenges associated with including pregnant subjects in imaging studies, especially those that involve ionizing radiation. To study the pudendal nerve stretch during vaginal delivery, Lien et al. [18] developed a female pelvic floor model consisting of the obturator internus muscles, piriformis muscle, coccygeal muscle, and sacrospinous ligament based on MRI images from a 34-year-old nulliparous, nonpregnant woman. Similarly, Hoyte et al. [19] modeled the levator ani muscles using

Downloaded from http://asmedigitalcollection.asme.org/biomechanical/article-pdf/143/5/050801/6641401/bio_143_05_050801.pdf by Michigan State University user on 11 March 2021

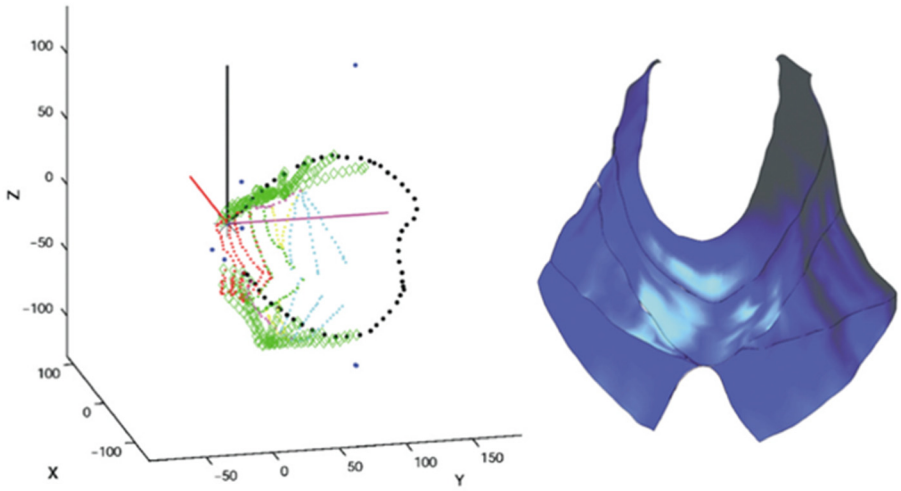

(*a*) (*b*)

Fig. 2 The 3D geometrical model of the pelvic musculature from a 72-year-old embalmed female cadaver. (*a*) Points for the 3D palpatory measurements. (*b*) Surface model of the pelvic floor muscles (pubococcygeus, iliococcygeus, and coccygeus) [33] (Reprinted with permission from Elsevier © 2003).

MRI images from a 21-year-old healthy, nulliparous, nonpregnant woman to evaluate the levator ani stretch during vaginal delivery. In addition, Yan et al. [16] constructed a model consisting of levator ani muscles, part of the obturator internus muscles, and the anterior pelvic bones—including the pubis and part of the ischium—based on MRI data from a healthy nulliparous, nonpregnant woman to study the influence of fetal head shape and size on the mechanics of childbirth. In contrast, Maran et al. [27] collected MRI images of seven pregnant women during the second stage of labor to describe the position changes of anatomical structures of the maternal pelvis and perineum. Pelvic floor muscles undergo large deformation during pregnancy. Therefore, MRI data collected close to the point of delivery would be of better accuracy to describe the pelvic floor structures for childbirth models.

In recent years, real-time MRI have been adopted to study childbirth-related topics. Compared to regular MRI, real-time MRI provides continuous monitoring of the observed objects, which is a beneficial feature for studying changes that happen to pelvic floor structures and the fetus during labor. Sindhwani et al. [31] used real-time MRI during the expulsion phase over two contractions to determine the stretch ratios in the levator ani muscle during childbirth. Bamberg et al. [32] evaluated the fetal head dimension changes—which occur due to fetal head molding—during the second stage of labor using the same technique. The studies conducted using real-time MRI can not only provide biofidelic measurements of anatomical structures during the delivery process that may be appropriate input to computational models but can also be used to validate the predictions of models that are developed.

Besides the in vivo data mentioned above, cadaveric data on anatomy have also been widely applied in the development of childbirth models. Janda et al. [33] measured geometric parameters of the pelvic floor muscles on an embalmed, 72-year-old female cadaver to investigate the relationship between MRI morphological data and palpatory morphological data. MRI measurements were performed first. Then the cadaver was dissected to reveal the pelvic floor muscle structures. 3D-palpation was used to measure the multiple types of markers placed on the pelvic floor muscles (Fig. 2). 3D geometrical models of the pelvic floor muscles that included the pubococcygeus, iliococcygeus, and coccygeus were created based on MRI data and palpatory measurements, respectively. The 3D geometrical models built from these two types of data sources exhibited good agreement on the pubococcygeus, iliococcygeus, and a large portion of the coccygeus. These cadaveric pelvic floor data were adopted into a modeling framework developed by Jorge's group and appeared in multiple studies [29,34–44]. Another major source of female pelvic floor cadaveric data is the visible human project. The visible human project is an effort by the U.S. National Library of Medicine to create a detailed dataset of photographs of human body cross section for the purpose of facilitating visualization of the anatomy. It provides a publicly accessible database of MRI, CT, and cross-sectional cryosection images obtained from one male cadaver and one female cadaver. Multiple childbirth models have referred to these data sets to develop their computational models. Gerikhanov et al. [23] used the pelvis data from the CT scan of the visible human project in their model, which simulated the cardinal movements of childbirth. In a study focusing on the contact algorithms needed for accurate childbirth models, Lapeer et al. [45] built the pelvis model based on visible human project data and determined the anatomy of the maternal soft tissues based on data from a 22-year-old from the BodyParts3D library, a Japanese database of MRI-acquired anatomical parameters. Routzong et al. [46] used frozen cryosection images from the visible human project to build the model of a maternal pelvis and pelvic floor muscles, including the levator ani and superficial perineal muscles, in an effort to determine the impact of superficial perineal structures on the pubovisceral muscle (also known as the pubococcygeus) and perineal body.

Thus, it can be seen that a range of database-informed and newly acquired anatomical data have been used to develop recent models of maternal pelvic anatomy for childbirth. Each has their limitations; however, clear documentation of the anatomical parameters will allow for more accurate comparisons between models and improved validation.

2.2 Fetal Anatomy and Biomechanical Characteristics. In comparison with the models of maternal pelvic floor muscles, which have been built based on detailed in vivo data, the fetal portion of computational birth models has been greatly simplified. Most fetal models only consist of a fetal head [11–14,16,17,21,23,25,26,31,46–53], fewer fetal models have a representation of the fetal body [20,29,34–40,42–44,54–56], and even fewer include articulation of any joint structures [22,45,57–59]. Even among those models that include the whole fetal body, generally only the delivery of the fetal head was simulated, not the whole

Downloaded from http://asmedigitalcollection.asme.org/biomechanical/article-pdf/143/5/050801/6641401/bio_143_05_050801.pdf by Michigan State University user on 11 March 2021

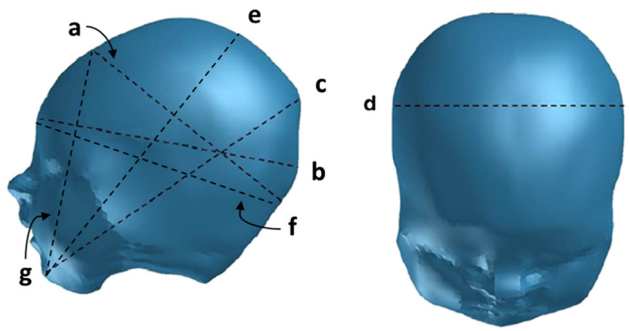

Fig. 3 A fetal head model based on MRI of a one-day-old neonate. The dimensions of the fetal head are measured by (*a*) suboccipitobregmatic diameter, (*b*) occipitofrontal diameter, (*c*) occipitomental diameter, (*d*) biparietal diameter, (*e*) mentovertical diameter, (*f*) suboccipitofrontal diameter, and (*g*) submentobregmatic diameter [25] (Licensed by Creative Commons CC BY 4.0). (Note: lines representing (*e*) mentovertical diameter, (*f*) suboccipitofrontal diameter, and (*g*) submentobregmatic diameter was added by authors of this review paper to the original figure from Krofta [25].).

body. The reason behind this modeling trend may be the fact that most childbirth models currently focus on maternal pelvic floor injuries, and it is reasonable to assume that—in a vertex position—passage of the fetal head puts the pelvic floor muscles into a state of higher strain and therefore at higher risk of injury compared to the passage of the body. This assumption has been made taking into consideration the viscoelastic properties of pelvic floor soft tissues, the fact that the fetal head is the first structure to exit the birth canal and the articulation of the fetal body. Head-only fetal models can be categorized into the following types: spherical models, ellipsoidal models, scanning models, and in vivo data-based models. With rare exceptions [31,47,48,50], these head-only models assumed nondeformable skulls (i.e., rigid materials or very high stiffness).

Spherical fetal head models are the simplest form, involving only one parameter: the diameter. Lien et al. [17] developed fetal head models with three diameters—80 mm, 90 mm, and 98.4 mm representing the 3rd, 50th, and 97th percentile fetal head, respectively—in order to study levator ani muscle stretch during vaginal childbirth. Noritomi et al. [11] and Berardi et al. [12] both used a 90 mm diameter for the spherical fetal head models in their studies that investigated the stress distribution in the levator ani muscle during labor.

As another form of simplified fetal head model, ellipsoidal models require two more diameters compared to spherical models. Sindhwani et al. [31] developed their ellipsoidal fetal head model with the long axis, craniocaudal axis, and left-right axis being 65.84 mm, 44.67 mm, and 44.33 mm, respectively, based on fitting ellipses to fetal head MRI images. Routzong et al. [46] constructed an ellipsoidal fetal head model with a circumference of 254.6 mm, without mentioning the length of the long axis. This significantly limits the ability of others to replicate the model, as circumference is not a deterministic parameter for an ellipse.

Three-dimensional scanning of skull physical models is another method commonly seen in fetal computational models [13,14,21,23,47,48,50–53,60,61], with improved biofidelity in shape and size compared to spherical and ellipsoidal head models. To improve the accuracy further, in vivo measurements are required. Krofta et al. [25] developed a fetal head model based on MRI of a one-day-old neonate, with critical diameters (Fig. 3) measured as: suboccipitobregmatic diameter = 100.3 mm, occipitofrontal diameter = 105.7 mm, occipitomental diameter = 131.9 mm, and biparietal diameter = 93.7 mm. In comparison, Oliveira et al. [49] developed their fetal head model without MRI, using critical diameters (Fig. 3) extracted from the literature directly (occipitofrontal diameter = 115 mm; submentobregmatic diameter = 95 mm; suboccipitofrontal diameter = 105 mm, and mentovertical diameter = 130 mm).

The Jorge group developed a whole fetal model in their modeling framework (Fig. 4(*a*)) [34]. The fetal head was constructed using critical diameters (suboccipitobregmatic diameter = 100 mm, suboccipitofrontal diameter = 105 mm, occipitofrontal diameter = 120 mm, mentovertical diameter = 130 mm, and submentobregmatic diameter = 115 mm, as shown in Fig. 3). The arms and legs were positioned in accordance with a full-term fetus. The whole fetal model was assigned a very high stiffness, without representation of the fetal joints. This fetal model later appeared in a series of studies [29,35–40,42–44,55]. In comparison, the whole fetal model developed by Buttin et al. [20] was simpler. The fetal head and fetal body were both made of ellipsoids and were assumed to be rigid, without dimensions being mentioned.

Fetal models with joint articulations are not common in the literature. Buttin et al. [22] constructed their fetal model with an ellipsoidal head and the body wrapped in an outer layer representing skin and other soft tissues (Fig. 4(*b*)). The neck articulation was achieved through the deformation and compressibility of the outer layer around the neck. As for mechanical properties of the fetal model, some contradictions exist: on one hand, the outer layer of soft tissues was described as having "a lower elasticity modulus"; on the other hand, the neo-Hookean material parameters for the outer layer, the skull, and the body were $C_{10} = 130$ KPa, $C_{10} = 75$ KPa, and $C_{10} = 70$ KPa, respectively. Improved fetal model geometry can be found in study by Lapeer et al. [45]. The fetal trunk of their model was from MRI scans of a

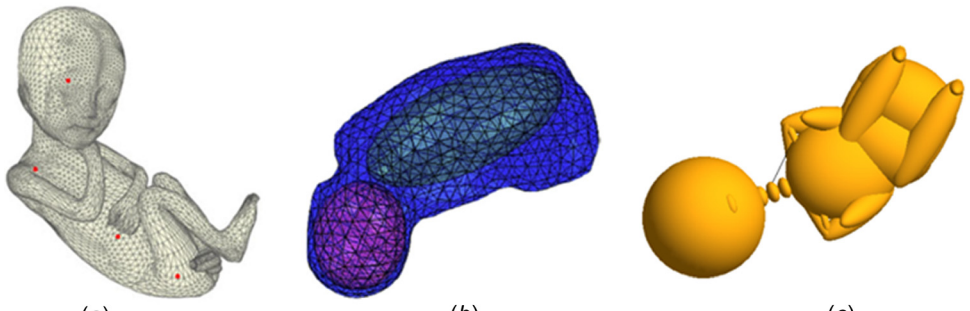

Fig. 4 (*a*) A fetal model with realistic head and body geometry, no representation of articulation [44] (Reprinted with permission from the John Wiley and Sons © 2017). (*b*) A fetal model consisting of skull, body, and outer layer soft tissues [22] (Reprinted with permission from Elsevier © 2013). (*c*) A fetal model with neck and shoulder articulation. The linear element running from the neck to the arm represents the brachial plexus [58].

Downloaded from http://asmedigitalcollection.asme.org/biomechanical/article-pdf/143/5/050801/6641401/bio_143_05_050801.pdf by Michigan State University user on 11 March 2021

stillborn, and the fetal head was from laser scanning of a skull replica. The neck articulation was modeled as a combination of linear and torsional springs, with parameter values of 100 N/m and 100 Nm/rad, respectively. The most complete representation of fetal articulations in the literature can be found in a framework developed by the Grimm group (Fig. 4(*c*)) [58,59], which was used to investigate shoulder dystocia–induced brachial plexus injuries. Their fetal model included both neck and shoulder articulations. Cervical vertebrae of the fetus were represented by seven ellipsoids, with axial and bending stiffness between each vertebral body defined based on experimental data from an infant caprine model [62]. Stiffness for the sternoclavicular and acromioclavicular joints of the fetal shoulder was defined at 2.5% of adult values, based on anatomical scaling. A nonlinear spring element was used to simulate the fetal brachial plexus on the left side, whose mechanical properties were represented with a bilinear function based on experimental data from rabbit tibial nerves [63]. The remainder of the joints of the upper and lower limbs were allowed to articulate, with joint stiffnesses based on the original MADYMO infant model, which were not necessarily biofidelic. As these joints were not involved with the occurrence or resolution of the shoulder dystocia, this was felt to be a reasonable simplification.

Despite the fact that modeling biofidelic fetal joint articulations requires considerable effort, it is critical to have this feature included in a childbirth model considering its significant role in the cardinal movements of labor. Parente et al. [42] compared three childbirth simulations with different degrees of neck flexion. Even with a rigid fetal model, they found that an increase in the degree of fetal head flexion is associated with lower values of forces that oppose the fetal descent as well as lower values of stress on the pelvic floor. As the fetus spontaneously and passively responds to the geometry of the birth canal through alterations in the relative position of the head, neck, and shoulders, allowing these structures to articulate is key to accurately simulating birth processes and the resulting biomechanical effects on the mother and infant.

2.3 Cardinal movements. The cardinal movements of the fetus during labor describe the multiple, critical fetal motions that help the fetus accommodate to the shape of the maternal pelvis and birth canal and thus exit with the least resistance. These movements include engagement, descent, flexion, internal rotation, extension, restitution, and expulsion [23]. Ideally, the fetal model in a childbirth simulation should be able to exhibit these movements with no imposed constraints—simply based on the interaction of the fetus and the maternal pelvis. Nonetheless, due to the limited biofidelity that computational models currently have (e.g., incomplete maternal soft tissues representation and lack of fetal neck articulation), the cardinal movements cannot be achieved spontaneously and the descent trajectory for the majority of fetal models is imposed during labor [23–25,64,65]. In the modeling framework developed by the Jorge group that was used in multiple studies [29,34–40,42–44], the trajectory of the fetal descent was imposed by applying displacements and rotations to several points along the fetal model (Fig. 4(*a*)). In another series of studies from the Nielsen group [13,16,21,26,51–53], the fetal descent trajectory was constrained by altering the vertical coordinates for the top nodes of the head, while in some cases rotation of the fetal head was permitted in order to produce less resistive force [52,53]. Gerikhanov et al. [23] studied the level of cardinal movements that could be achieved when different numbers of guiding waypoints were imposed along the fetal descent trajectory. They found that at least three waypoints had to be applied for the fetus to exhibit all seven cardinal movements within their pelvis-only maternal structures. Their results addressed the importance of inclusion of full fetal articulation and maternal soft tissues in arriving at a realistic, forward-engineered, human childbirth computational model.

In an effort to model childbirth without an imposed trajectory, Buttin et al. [22] built a computational model that included the fetus, uterus, abdomen, and pelvis. The delivery was driven by simulated cyclic uterine contractions and voluntary maternal efforts. A slight pressure was added inside of the abdomen to represent residual maternal muscle tone. The inclusion of the uterus and abdomen environment enabled the simulation of uterine contractions and maternal pushing and helped to restrict the movement of the fetus. However, the lack of realistic neck and shoulder articulations limited the model's ability to achieve full cardinal movements. Lapeer et al. [45] investigated the influence of pelvic floor soft tissues on the cardinal movements of the fetus. By modeling the maternal pelvis, the uterine cervix, and a whole fetus, Lapeer and colleagues conducted four simulations to examine the number of cardinal movements achieved when different soft tissues (levator ani and sacrospinous ligaments) were involved. They found that only when levator ani muscles and sacrospinous ligaments were both included, all four cardinal movements in the study (flexion, internal rotation, extension, and restitution) could be obtained. Although shoulder articulation was still missing in their study, the more realistic fetal model (based on laser scanning and MRI data), the improved pelvic floor structures, and the model's contact methods helped this study to gain advantage over previous studies in achieving more biofidelic fetal movements.

2.4 Maternal soft Tissue Mechanical Behavior. The maternal soft tissues related to childbirth are those of the pelvic floor, the perineum, and the pelvic organs. The pelvic floor provides crucial support to the pelvic organs, including the uterus, cervix, vagina, bladder, and rectum (Fig. 1). The pelvic floor undergoes large stretches during delivery. It is responsible for a significant portion of the resistive force that the fetus experiences and is at significant risk of injury [2]. The key pelvic organs include the soft tissues (i.e., uterus, cervix, and vagina) that are in direct contact with the fetus. Uterine contraction is a primary source of the delivery force. The uterus and vagina define the birth canal for fetal passage, and dilation of the cervix is a key adaptation process during the first stage of labor. Accurate and comprehensive descriptions of these maternal soft tissues are critical in simulating the cardinal movements of the fetus and evaluating the risk of injuries for both the mother and the child. The pelvic floor includes the pelvic diaphragm, the perineal membrane, and the deep perineal pouch. The levator ani muscles of the pelvic diaphragm are the most commonly included maternal soft tissues in childbirth models, while pelvic organs are not commonly modeled in these studies.

Based on the level of comprehensiveness, pelvic floor soft tissue properties found in the literature can be grouped as follows: isotropic, nonlinear materials; anisotropic, nonlinear materials; and viscoelastic, anisotropic, nonlinear materials.

For the isotropic, nonlinear material group, a neo-Hookean model [13,22,45] or a Mooney–Rivlin model [11,14] are popular choices. The Ogden material can also been found in the literature [25]. These models are well established within soft tissue biomechanics. Material parameters in these studies were derived from uniaxial or biaxial tensile test of human or animal soft tissue specimens (e.g., human tongue tissues from surgery, human cadaveric pelvic floor tissues, and canine heart left ventricle tissues). More uniquely, Yan et al. [16] applied an isotropic, exponential constitutive equation, as shown in Eq. (1), to describe the mechanical behavior of pelvic floor muscles

$$\Psi = a\left[e^{b(I_1-3)} - 1\right] \tag{1}$$

where I_1 was the first invariant of the right Cauchy–Green deformation tensor. The material parameters a and b were obtained by fitting the constitutive equation to the uniaxial tension experimental data of fresh human pelvic floor muscle specimens.

Downloaded from http://asmedigitalcollection.asme.org/biomechanical/article-pdf/143/5/050801/6641401/bio_143_05_050801.pdf by Michigan State University user on 11 March 2021

When it comes to anisotropic, nonlinear material models, fibers will normally be added to introduce the transversely isotropic properties. Li et al. [21] used the following strain energy function to describe the mechanical properties of levator ani muscles:

$$\Psi = \left(1-\alpha\right)a\left[e^{b(I_1-3)}-1\right]+\alpha c\left[e^{d(\lambda^f-1)^2}-1\right] \tag{2}$$

where I_1 was the first invariant of the right Cauchy–Green deformation tensor; λ^f was the stretch ratio in the fiber direction; and a, b, c, d were material parameters to be determined from experimental data. The parameter α was introduced to change the cross-fiber direction stiffness and thus to adjust the anisotropy level of the material. They used four different α values (0, 0.2, 0.5, 0.8) to determine the influence of anisotropy levels on the peak force and maximum stretch of the levator ani muscle during childbirth. Berardi et al. [12] used the Holzapfel strain energy function to represent the levator ani muscle's mechanical behavior, written as

$$\Psi = c_{10}(I_1-3)+\frac{k_1}{2k_2}\left[e^{k_2(E_\alpha)^2}-1\right]+\frac{1}{D}\left(\frac{J_{el}^2-1}{2}-\ln J_{el}\right) \tag{3}$$

where I_1 was the first invariant of the right Cauchy–Green deformation tensor; J_{el} was the elastic volume ratio; E_α was a strain-like quantity that characterizes the deformation in the direction of the fibers; and c_{10}, k_1, k_2, D were material parameters. The strain energy functions used in a series of studies by Oliveira and colleagues [36,39,40] were similar to Li et al. [21], with extra parameters introduced to represent tissue damage. Their strain energy function was written as

$$\Psi = (1-D_m)\Psi_{\mathrm{I}}(I_1)+(1-D_f)\Psi_{\mathrm{f_{PE}}}(\lambda^f)+\Psi_{\mathrm{J}}(\mathrm{J}) \tag{4}$$

where $\Psi_{\mathrm{I}}(I_1)=a\left[e^{b(I_1-3)}-1\right]$ represented the isotropic ground matrix; $\Psi_{\mathrm{f_{PE}}}=c\left[e^{d(\lambda^f-1)^2}-1\right]$ represented passive mechanical properties of muscle fibers, with the same letter meanings as in Eq. (2); $\Psi_{\mathrm{J}}(\mathrm{J})$ represented the volumetric contribution and enforced incompressibility, where J was the volume ratio; D_m and D_f were damage variables ranging between 0 and 1, which indicated undamaged and maximal amount of damage; and D_m and D_f were determined by variables associated with strain energies at initial and total damage.

The same author group added the Maxwell model to the constitutive model in Eq. (4) to describe the viscoelastic, anisotropic, nonlinear mechanical behavior of soft tissues [43,44], written as

$$\Psi = \Psi_{\mathrm{I}}(I_1)+\Psi_{\mathrm{f_{PE}}}(\lambda^f)+\Psi_{\mathrm{J}}(\mathrm{J})+\Psi_{\mathrm{VSC}}(\alpha,\mathbf{C},\mathbf{\Gamma}) \tag{5}$$

where $\Psi_{\mathrm{VSC}}\left(\alpha,\mathbf{C},\mathbf{\Gamma}\right)=\sum_{\alpha=1}^{m}Y_\alpha(\mathbf{C},\mathbf{\Gamma_\alpha})$, represents $\alpha=1,2,\ldots m$ parallel elements added to the elastic part of the material; each viscoelastic element was represented by a spring in series with a dashpot; Y_α represented the dissipative potential, which was a function of the isochoric part of the internal variables $\mathbf{\Gamma_\alpha}$, and the Cauchy–Green deformation tensor $\mathbf{C}$. Each viscoelastic process was characterized by two mechanical properties: the free-energy parameters β_α and the relaxation time τ_α. This constitutive model still allows the damage variables D_m, D_f, as shown in Eq. (4), to be added to Eq. (5) for damage evaluation.

The need for the complexity and biofidelity in modeling the tissues of the pelvic floor may depend on the goal of the model. Unfortunately, there has not yet been a systematic, parametric analysis comparing the predictions of birth-related outcomes for either the mother or the fetus based on different formulations of the maternal tissue properties (with all other parameters held constant). Thus, there currently is no guidance for researchers on when the increased modeling complexity is warranted—and when it is not.

3 Applications of Childbirth Models

3.1 Childbirth characteristics. Childbirth is a complex mechanical process with unique characteristics. Uterine contractions along with maternal pushing generate an outward delivery force that leads to descent of the fetus. The dilation of the cervix eases the passage of the fetal head along the birth canal. The pressure from the birth canal molds the fetal head into an oblong shape, while the overlapping of the bones of the skull at the sutures makes it easier for the head to pass through the birth canal. Increased knowledge of the process of fetal head molding will improve our understanding of fetal head structural integrity and neonatal facial soft tissue injuries. During the birth process, if any of the cardinal movements put the fetus into an abnormal position, risk of injuries will increase for both the mother and the neonate. In this section, we will discuss computational studies that contribute to improved understanding of the process of childbirth itself.

Bailet et al. [48] developed a model to quantify the fetal head deformation during childbirth. The fetal head geometry was based on 3D scanning from a medical manikin. The fetal skull was described by a linear elastic material, with a Young's modulus of 7.23 MPa for the fontanels and suture area and a Young's modulus of 2.65 GPa for the cranial bones. A pressure of 45 kPa was applied across the diameter of the fetal head to simulate the circumferential pressure resulting from passage through the birth canal. They recorded an increase of the maxillo-vertical diameter and the orbito-vertical diameter (1.29 mm increase from 124.6 mm, and 1.13 mm increase from 110.9 mm, respectively), and a decrease of the suboccipitobregmatic diameter (3.57 mm decrease from 107.4 mm). These geometry changes align with a previous photographic study [66] and a numerical study on fetal head molding [67].

To understand the role that pelvic floor muscles play in the magnitude of the required delivery force, Li et al. [13] compared delivery forces between athlete and nonathlete parturients. Levator ani muscle geometry of an athlete and a nonathlete were obtained through MRI. An incomplete fetal head model was built by laser scanning a skull replica, representing the vault of the fetal head without the front facial structure. The pelvic floor muscles and the fetal head were both described with incompressible, isotropic, neo-Hookean materials, with the fetal head assigned a high stiffness parameter. Their study showed a 45% increase in required force to achieve delivery for the athlete compared to the nonathlete. Meanwhile, the levator ani muscles reached similar stretch ratio peak values for the athlete and nonathlete (3.25 and 3.20, respectively). It is worth noting that their study only accounted for geometric differences in the levator ani and did not include any differences in the soft tissue mechanical properties between the athlete and nonathlete subjects. This could either widen or narrow the delivery force differences found in their study. Parente et al. [37] further explored the influence of the mechanical behavior of the pelvic floor muscles on delivery force. Using the same framework mentioned above [34], Parente et al. estimated the influence of pelvic floor muscle activation during vaginal delivery. The opposing (resisting) forces against fetal descent and the stress within the pelvic floor muscles were obtained in four different pelvic floor muscle activation levels: 0% (i.e., passive state), 5%, 10%, and 15%. The average stress was evaluated on a curve passing along the bottom of the pubococcygeus muscle, which was previously determined to be the high stress area during vaginal delivery. Results showed that the increase in pelvic floor muscle activation was followed by higher opposing forces to resist fetal descent and higher values of pelvic floor stress.

During the internal rotation stage of the cardinal movements, the fetal head transitions from an occipito-transverse position to an occipito-anterior position (fetal head facing the mother's back) in most cases. In a smaller number of deliveries, the fetal head turns into an occipito-posterior position (fetal head facing the mother's abdomen) [68]. Parente et al. [38] verified the effect of

Downloaded from http://asmedigitalcollection.asme.org/biomechanical/article-pdf/143/5/050801/6641401/bio_143_05_050801.pdf by Michigan State University user on 11 March 2021

an occipito-posterior position of the fetus during delivery on the stretch values of the pelvic musculature when compared to the normal occipito-anterior position. Using their previously developed framework [34], they showed that the occipito-posterior position would induce a higher maximum stretch in the levator ani muscle compared to the occipito-anterior position (maximum stretch ratio: 1.73 versus 1.63). These results addressed the significant role of cardinal movements—and their variation—in facilitating the passage of fetus through the birth canal.

Li et al. [14] investigated the effect of different levels of constraint on fetal head motion on the mechanical response of the pelvic floor muscles using their previously developed modeling framework [13]. Three different types of fetal head constraints were compared: (1) a completely prescribed head path; (2) a partially constrained head, allowing rotation about one point on the head; and (3) a minimally constrained head, allowing both rotation and translation. Results showed that the minimally constrained head required a much lower total force to achieve delivery. The maximum principal stretch ratio was found at the same location (i.e., the right levator ani attachment point to the pubis) for all three cases. Case 1 and case 2 induced the same amount of stretch (stretch value 2.6), while case 3 was responsible for a slightly higher value (stretch value 2.7). Thus, the more biofidelic model (allowing free fetal head motion) showed a reduction in the necessary force to achieve delivery, but a greater amount of stretch in the pelvic muscles. This again points to the importance of striving for biofidelic models in order to accurately understand the mechanics of the birth process—and hopefully to determine which opposing factors (e.g., amount of needed delivery force versus degree of stretch) are most relevant in terms of predicting injury risk and/or labor difficulties.

3.2 Maternal Injuries. Childbirth can lead to maternal injuries in the perineal area and the pelvic floor. Computational models that investigate maternal childbirth injuries primarily focus on pelvic floor injuries. The pelvic floor muscles surround the birth canal and experience large deformations during the childbirth process, which introduces significant risk of permanent structural damage and injury [2]. With weakened pelvic floor muscles, the patient may experience urinary and fecal incontinence along with persistent postpartum pain in the short term and potential pelvic organ prolapse in the long term [69].

The peak stretch and stress that pelvic floor muscles experience during childbirth are of great interest within numerical studies [11,12,29,34,35], since stretch and stress are indices directly related to muscle injuries and are hard to evaluate through other means. Martins et al. [34] presented a finite element modeling framework to simulate the active deformation of the levator ani muscle under constant pressure and deformation induced by vaginal childbirth. Their model was comprised of a levator ani based on data from a 72-year-old cadaver and a geometrically realistic fetal model (modeled as a rigid body with high stiffness). The pelvic floor muscle mechanical behavior was described by a transversely, isotropic material with a single fiber direction embedded in an isotropic matrix. Their simulation of the activation of the levator ani muscle (to simulate active muscle properties in comparison to passive properties) revealed that muscle activation opposed the widening of the urogenital hiatus when pressure was applied to the inner surface of the levator ani. When the muscle was passively submitted to a pressure, the sling attachment points of the levator ani were the regions where maximum stress occurred. These are regions where most postpartum lesions occur in real life. When a delivery of the fetus was simulated in their study, the maximum stretch value was 1.6 on a circumferentially defined path at the pubococcygeus region.

Using the same framework, Parente et al. [35] defined seven different trajectories in the circumferential direction on the levator ani to facilitate the quantification of stretch and strain during childbirth. Their study showed the evolution of the strain along different trajectories on the levator ani during the process of fetal descent. They concluded that for a fetal head vertical displacement of 60 mm, the maximum stretch ratio of 1.63 was achieved at the lowest trajectory along the edge of pubococcygeus.

Noritomi et al. [11] developed a pelvic floor muscle finite element model based on in vivo MRI images. They simulated the passage of the fetal head through the pelvic floor using a spherical fetal head model under quasi-static movement and concluded that high stress areas during childbirth are located on the pubococcygeus muscle and the tendinous arch region. Investigating the same question, a study from Berardi et al. [12] also supported the conclusions that the maximum deformation and stress are found in the pubococcygeus muscle. The maximum deformation (stretch ratio) and stress obtained in their study was 2.2 and 17 MPa, respectively.

Silva et al. [29] further investigated the influence of fetal head molding on the pelvic floor muscles during childbirth. Their study compared the passage of two fetal models through pelvic floor muscles, one with a rigid head and one with a deformable head. The deformable fetal head included the following structures: skin and soft tissues ($E = 0.3$ MPa, $\nu = 0.25$), skull ($E = 250$ MPa, $\nu = 0.22$), brain ($E = 0.0246$ MPa, $\nu = 0.49$), fontanels and sutures ($E = 3.8$ MPa, $\nu = 0.49$). Results showed that delivery of a fetus with a deformable head, which is more representative of the real world, had a significant impact on the resistive forces provided by the pelvic floor muscles—reducing them by 17.3% (26 N versus 30.5 N). However, the reduction in the maximum stretch in the levator ani was only 1.86%—indicating that even when the fetal head deforms, there is significant stretch occurring within the muscle. These results illustrate how modeling details in a complex system can affect the final outcomes.

Under the same framework shown in Martins et al. [34], Oliveira et al. [36] introduced two damage variables into the strain energy function for the levator ani muscle to account for the damage level. They concluded that the injuries during delivery were localized in the middle part of the muscles, in its attachment and the region of connection with the arcus tendineus. They also concluded that puborectalis component of the levator ani muscle was the most prone to damage. However, their model did not include a

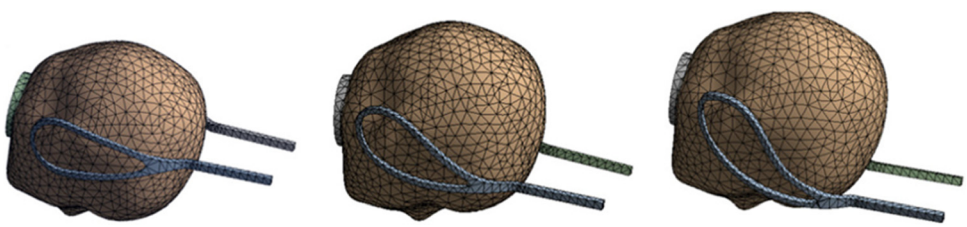

Fig. 5 Forceps delivery simulation with different angles of the forceps blades: (*a*) 0 deg, (*b*) 20 deg, and (*c*) 40 deg [70] (Reprinted with permission from World Scientific Publishing Co., Inc. © 2000)

Downloaded from http://asmedigitalcollection.asme.org/biomechanical/article-pdf/143/5/050801/6641401/bio_143_05_050801.pdf by Michigan State University user on 11 March 2021

puborectalis component, such that the part of levator ani enduring the most damage in their study was actually the pubococcygeus muscle.

While stretch in the pelvic muscles has been the primary focus of computational childbirth models over the past 30 years, the primary conclusions that can currently be drawn are which regions of the tissue are likely to see the greatest amount of stretch. However, as the models are neither generally biofidelic nor patient-specific, they have not yet allowed for the development of mitigation strategies or personalized risk assessments for patients.

3.3 Fetal Injuries. Very few childbirth computational models that focus on fetal injuries could be found in the literature. The studies available are focused on two types of injuries: fetal head injuries associated with operative vaginal delivery [47,60,70] and shoulder dystocia related brachial plexus injuries [58,59].

Forceps delivery and vacuum delivery are the two most common types of operative vaginal delivery. Forceps are scissors-like devices with spoon-shaped blades designed to apply traction on the fetal head to guide it out of the birth canal. Vacuum delivery uses the traction generated by the vacuum between a small cup and the fetal head to assist with extraction of the fetus from birth canal. Operative deliveries may be undertaken during a difficult labor, to supplement ineffective delivery forces from uterine contractions and maternal pushing, as an alternative to the more invasive cesarean delivery, which requires incisions in the abdomen and uterus. Operative delivery can cause fetal injuries like bruising, facial nerve injuries, cephalohematoma, retinal bleeding, skull fracture, etc. [71,72]. These injuries may be caused by the pressure exerted by the forceps or the vacuum cup on the fetal head. Computational modeling is a perfect tool to explore proper protocols for operative vaginal delivery.

To understand how the curve angle of forceps blades and the material they are manufactured from would affect the neonatal neck stress and pressure during childbirth, Su et al. [70] developed a finite element model of the fetal scalp and skull with reference to an anatomical head model and skull model of a newborn. Six pairs of forceps with three different blade curve angles (20 deg, 40 deg, 60 deg) and two material types (stainless steel and titanium alloy) were constructed within the model software (Fig. 5). Forceps operative deliveries with 10 N of clamping force and 100 N of extraction force were applied on the fetal head. They found that a larger curve angle of the blades of the forceps decreased the stress on the fetal neck but could lead to rotation toward the posterior aspect of the head (elevating the chin). Moreover, forceps made of a lower Young's modulus material (titanium alloy) also reduced the stress on the fetal neck. In order to link the options in the design of forceps to a reduction in injury risk, specific links between neck stress and head rotation and the mechanisms of injury are still needed. But these models demonstrate how computational modeling can be used to support clinical decision-making and biomedical engineering design.

In another attempt to understand the impact of forceps delivery, Lapeer et al. [47] and colleagues compared the deformation of and stress on the fetal head under different forceps placements. Through laser scanning of a skull model, they constructed a fetal head finite element model that contained the skull base, the maxilla, the fetal cranial bones, and the fontanels. The fetal cranial bone was modeled as an orthotropic material with two Young's moduli, while the other three parts were modeled as an isotropic material with a single Young's modulus. The forceps were applied with either symmetric or asymmetric placement with 120 N of clamping force and 200 N of traction force. The study found that asymmetric placements exhibited higher amounts of deformation and shear stresses, for both average values and peak values. Using the same framework, their group also assessed quantitatively if incorrect placement of a vacuum cap would cause serious injury to the fetal scalp [60]. Vacuum pressure of 66.7 kPa with a maximum allowable traction of 131 N was used on both correct placement (in between the anterior and posterior fontanels) and incorrect placement (across the anterior fontanel) of the vacuum cup on the fetal skull (Fig. 6). They found that direct placement across the soft, anterior fontanel was associated with significantly higher deformations across the contact area. This deformation may then be related to vascular disruptions (and bleeding) in either the extradural or subdural blood vessels.

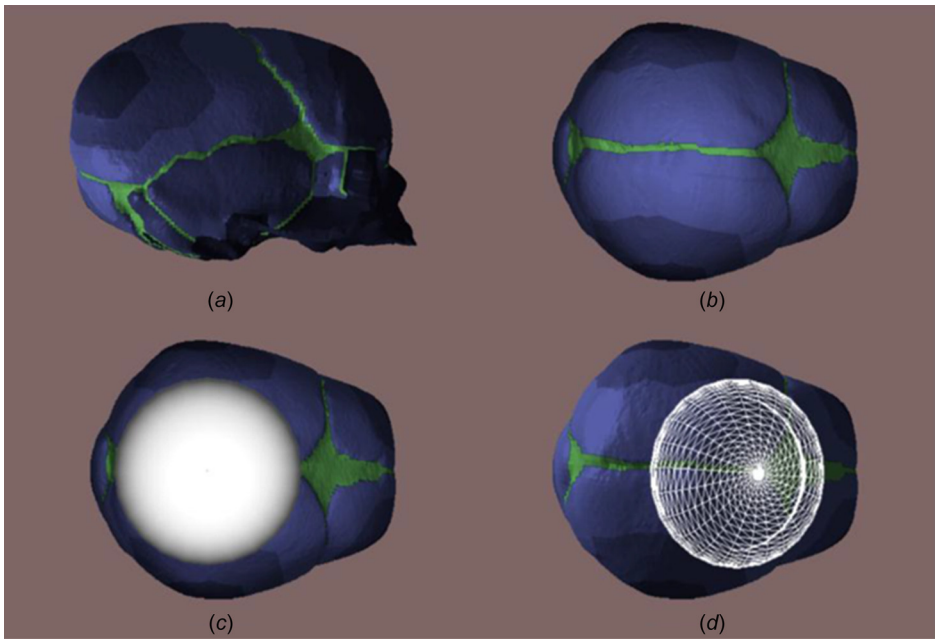

Fig. 6 A computational fetal head model based on data of laser scanning of a physical fetal head model. Side view (*a*) and top view (*b*) of the fetal head model are shown. Cranial bones, fontanels, and sutures are included in the model. The correct placement (*c*) and the incorrect placement (*d*) of the suction cup are shown [60]. Reprinted with permission from the *SIMULIA Regional User Meeting RUM 2014*.

Downloaded from http://asmedigitalcollection.asme.org/biomechanical/article-pdf/143/5/050801/6641401/bio_143_05_050801.pdf by Michigan State University user on 11 March 2021

The brachial plexus is a network of nerves that travel from the spinal cord in the neck down to the arm. A newborn may sustain brachial plexus injury during or even before childbirth. From a biomechanical perspective, the direct cause of NBPP is the overstretch of the brachial plexus resulting in rupture or avulsion of the nerve roots of the plexus (C5–T1). During labor, if impact between the fetal shoulder and the maternal pelvis occurs such that the shoulder is restrained, the forces that work to achieve delivery can continue to advance the infant's spine, neck, and head further down to birth canal and widen the angle between the neck and the shoulder. This can occur through both uterine contractions and maternal pushing efforts as well as clinician-applied traction. This widening of the neck/shoulder angle will cause the brachial plexus to stretch—and if the stretch that occurs is greater than the nerve root injury threshold, permanent injury can occur. A lesser amount of stretch can result in substructural damage that can result in a temporary injury, which may require up to 12 months to recover. As a significant risk factor for neonatal brachial plexus injuries, shoulder dystocia has been studied using computational models. Gonik et al. [58] simulated a shoulder dystocia event using a framework that included a fetal model with fully articulated neck and shoulder to investigate the impact of the type of delivery forces and the pelvic angle on brachial plexus stretching. Their model started with the impaction between fetal anterior shoulder and the maternal pubic symphysis, after the fetal head was delivered. Two types of delivery forces (maternal endogenous forces and clinician-applied exogenous forces) and three pelvic angles (angle between pubic symphysis and the horizontal plane: 45 deg for lithotomy positioning, 30 deg and 20 deg for McRoberts' positioning) were simulated. Delivery forces and brachial plexus stretching (measured in nominal strain) were evaluated for each one of the seven delivery scenarios, among which one scenario allowed fetal neck lateral flexion under exogenous delivery force and lithotomy positioning, while other cases had the fetal neck axially fixed. Results showed that McRoberts' positioning reduced delivery force for both the endogenous delivery force scenario and the exogenous delivery force scenario (up to 37% and 47%, respectively). The more aggressive McRoberts' positioning tilting angle (by changing from 30 deg to 20 deg) further reduced delivery force under the exogenous delivery force scenario but did not reduce delivery force under the endogenous delivery force scenario. The fetal neck lateral flexion did not increase the exogenous delivery force much (75 N–80 N), but increased brachial plexus stretching significantly (strain values from 14% to 18.2%). McRoberts' positioning is associated with lower brachial plexus stretching, with the more aggressive pelvic tilting angle lowering the brachial plexus stretch even more, for both types of delivery forces. One interesting finding from the results was that with the same pelvis tilting angle, maternal endogenous force could lead to higher brachial plexus stretching compared to delivery under clinician-applied exogenous force, which suggested that clinician-applied exogenous force was not by default the source of brachial plexus injuries.

3.4 Protective Measures During Delivery. In order to minimize the trauma that childbirth induces on both the mother and the child, various protective measures have been developed for both mothers and neonates during the management of difficult labors. Computational models serve as a powerful tool to verify the effectiveness of these measures and to explore improvement through newly designed measures.

Jansova et al. [64] verified whether a manual perineal protection technique can reduce perineal tension during delivery in comparison with the hands-off technique. Maternal perineal structures consisting of the pubis, inferior pubic rami, genital hiatus, perineal body, and anus were modeled based on clinical measurements. The descent of the fetal head, a spherical model with a diameter of 9.5 cm, was simulated as a quasi-static movement following the curve of Carus, an imaginary arc corresponding to the pelvic axis [73]. The soft tissue mechanical behavior was described using a transversely isotropic, hyperelastic, Mooney–Rivlin material. Two perineal protection methods—with different fingertip distances (10 cm and 11 cm)—were compared to the hands-off method. Their study showed that both manual perineal protection methods significantly reduced both the peak stress values (39% drop for 10 cm fingertips distance, and 30% drop for 11 cm fingertips distance) and the area exposed to high stress levels (10 cm distance: 10% high stress area, 11 cm distance: 15% high stress area, hands-off: 30% high stress area) compared to the hands-off method. Using the same framework, their group later evaluated the order of effectiveness of 10 different manual perineal protection methods for three sizes of fetal head [65]. Small, average, and large fetal heads were defined based on the biparietal diameter and suboccipitobregmatic diameter. Results showed that the level of effectiveness of the studied manual perineal protection methods were nearly identical for fetal heads of all three sizes. The most effective method was described as "the fingertips being initially placed 12 cm apart and 2 cm anterior from the posterior fourchette, and with a subsequent movement one cm on each side toward the midline without any anterior–posterior shift." The study also suggested that manual perineal protection should be performed as a common measure in all deliveries instead of being reserved only for deliveries with a higher risk (i.e., macrosomic fetuses).

During difficult labors, an episiotomy—surgical incision of the tissues between the vaginal opening and the anus—may need to be performed to facilitate the delivery. Oliveira et al. [39] evaluated the protective effect of a mediolateral episiotomy by assessing principle stress, antero-posterior reaction force, and damage to the pelvic floor muscle. With a previously developed modeling framework—that has maternal pelvic structures based on data from a 72-year-old cadaver, a fetal model with realistic head and body geometry, and pelvic floor muscle mechanical behavior described as a transversely isotropic material with a single fiber family embedded in an isotropic matrix—their study compared mediolateral episiotomies with an incision length of 10 mm, 20 mm, and 30 mm and incision angles of 30 deg, 45 deg, and 60 deg from the vertical. Their study concluded that the angle of the incision affected the amount of stress measured in the pelvic floor muscles and that 30 deg is the most protective angle for an episiotomy. As to the length of the incision, the longer the incision was, the lower the force that was required to achieve delivery and the lower the predicted pelvic muscle damage was during a normal delivery. When the location of the damage was evaluated, the induced damage was confined to the upper edge of the incision, which was much smaller than the damaged area without episiotomy. The same group of researchers [40] later investigated the influence of mediolateral episiotomies on the pelvic floor mechanics comparing the occiput posterior position to the more common occiput anterior position. They found that 10 mm incision lengths were the ones that resulted in the higher amount of resistive force, and 30 deg angles were the ones that lead to greater incision enlargement. Compared to the occiput anterior fetal head position, the occiput posterior position induced: (1) higher resistive force; (2) higher stresses; (3) larger enlargement of the levator ani outlet diameter; (4) and higher growth of damage. In another study that compared the effectiveness of different episiotomy strategies, Oliveira et al. [49] compared the damage reduction effectiveness (on the pelvic musculature) of multiple incisions (double and triple) with different angle (30 deg, 45 deg, 60 deg) and location (left and right side) combinations to double and triple-length single incisions. Results showed that two incisions did not reduce the damage as effectively as a double-length, single incision. Moreover, longer incisions were also more effective in reducing delivery force: delivery with the longest episiotomy incision in the study (a 30-mm incision) had the lowest magnitude of resisting force (42.0 N) during the fetal descent, while delivery without episiotomy had the highest magnitude of resisting force (68.8 N). Therefore, a single, longer episiotomy incision was more favorable than

Downloaded from http://asmedigitalcollection.asme.org/biomechanical/article-pdf/143/5/050801/6641401/bio_143_05_050801.pdf by Michigan State University user on 11 March 2021

Table 1 Characteristics of maternal and fetal models in childbirth computational studies

Authors	Imaging technique	Maternal model	Fetal model	Maternal soft tissue mechanical properties	Fetal model mechanical properties	Fetal descent path
The Grimm group [58,59]	N/A	Pelvis.	Whole fetal model, including neck and shoulder anatomical structures and articulation, and BP.	N/A	Neck and shoulder: biofidelic articulation. BP: bilinear tensile properties.	Not imposed.
Lien et al. [17,18]	Maternal: MRI.	Pudendal nerve, OBI, piriformis, and coccygeus [18]. Pelvic bone. LA, TALA, urethra, lower vagina, internal and external anal sphincters [17,18].	Head only, spherical.	N/A	N/A	Imposed, the curve of Carus.
The Jorge group [29,34–40,42–44]	Maternal: MRI and dissection from Janda et al. [33].	Pelvis, LA (without puborectalis), coccygeus, OBI, and TALA.	Whole fetal model with realistic geometry, no articulation. Head dimensions are measured by "a,", "b,", "f," "e," and "g" shown in Fig. 3.	Transversely isotropic nonlinear material: one muscle fiber family is embedded in an isotropic matrix. Active traction of the muscle fiber [29,34,41], variables representing tissue damage [36,39,40], and Maxwell model representing viscoelastic properties [43,44] can be added.	Nondeformable.	Imposed, by applying displacements and rotations to one or several reference points on the fetal model.
Hoyte et al. [19]	Maternal: MRI.	Pelvis, LA, and OBI.	Head only, spherical.	Isotropic, nonlinear material. Modified Saint Venant–Kirchhoff model.	Nondeformable.	Imposed, along the path of vagina.
Li et al. [13]	Maternal: MRI. Fetal: laser scanning.	LA and OBI.	Head only, incomplete, including the vault of skull.	Isotropic nonlinear material. Neo-Hookean model.	Nondeformable.	Imposed.
Buttin et al. [20]	Maternal: MRI.	Uterus, birth canal, and amniotic liquid.	Head and body. No articulation.	Isotropic linear elastic material.	Nondeformable.	Not imposed.
Li et al. [14]	Maternal: MRI. Fetal: laser scanning.	LA and pubis.	Head only, incomplete, including the vault of skull.	Isotropic nonlinear material. Mooney–Rivlin model.	Nondeformable.	Imposed, three scenarios.
Li et al. [21]	Maternal: MRI. Fetal: laser scanning.	LA and OBI.	Head only, incomplete, including the vault of skull.	Transversely isotropic nonlinear material. Material model is shown in Eq. (2).	Nondeformable.	Imposed, vertical descent path is prescribed, free to rotate and translate.
Buttin et al. [22]	Maternal: MRI, CT.	Pelvis, uterus, and abdomen.	Head, body, and skin tissues. Articulated neck.	Isotropic nonlinear material. Neo-Hookean model.	Nondeformable.	Not imposed.
Gerikhanov et al. [23]	Maternal: CT from VHP. Fetal: laser scanning.	Pelvis.	Head only.	N/A	Nondeformable.	Imposed, zero to three guiding points along the trajectory.
Noritomi et al. [11]	Maternal: MRI.	Pelvis, LA, and coccygeus.	Head only, spherical.	Isotropic nonlinear material. Mooney–Rivlin model.	Nondeformable.	Imposed, straight movement.
Berardi et al. [12]	Maternal: MRI.	Pelvis and LA (without puborectalis).	Heading only, spherical.	Anisotropic nonlinear material. Holzapfel model, as shown in Eq. (3).	Nondeformable.	Imposed, vertical translation.

Downloaded from http://asmedigitalcollection.asme.org/biomechanical/article-pdf/143/5/050801/6641401/bio_143_05_050801.pdf by Michigan State University user on 11 March 2021

Table 1 (continued)

Authors	Imaging technique	Maternal model	Fetal model	Maternal soft tissue mechanical properties	Fetal model mechanical properties	Fetal descent path
Lapeer et al. [47,60]	Fetal: laser scanning.	N/A	Head only, including the skull base, the maxilla, the cranial bones, and the fontanels.	N/A	Cranial bone: orthotropic linear elastic material. The rest: isotropic linear elastic material.	N/A
Jansova et al. [64,65]	N/A	Pubis, inferior pubic rami, perineum, and anus.	Head only, spherical [64] or dimensions measured by "a" and "d" shown in Fig. 3 [65].	Transversely isotropic nonlinear material. Trans-iso-Mooney–Rivlin model.	Nondeformable.	Imposed, the curve of Carus.
Bailet et al. [48]	Fetal: 3D scanning.	N/A	Head only.	N/A	Linear elastic material.	N/A
Yan et al. [16]	Maternal: MRI. Fetal: CT.	LA, part of OBI, pubis, and part of the ischium.	Head only.	Isotropic nonlinear material. Exponential strain energy density function.	Nondeformable.	Imposed.
Su et al. [70]	N/A	N/A	Head only.	N/A	Scalp: linearly elastic material. Skull: Nondeformable.	N/A
Sindhwani et al. [31]	Maternal and fetal: MRI and live MRI.	LA.	Head only, ellipsoidal.	N/A	Deformable, based on live MRI.	Imposed, based on live MRI.
Krofta et al. [25]	Maternal and fetal: MRI.	Pelvis, OBI, and LA.	Head only, dimensions measured by "a," "b," "c," and "d" shown in Fig. 3.	Isotropic nonlinear material. Ogden model.	Nondeformable.	Imposed, the curve of Carus.
Routzong et al. [46]	Maternal: cryosection data from VHP.	Pelvis, LA, and superficial perineal muscles.	Head only, ellipsoidal.	Isotropic nonlinear material. Neo-Hookean model.	Nondeformable.	Imposed.
Lapeer et al. [45]	Material: VHP and BodyParts3D library. Fetal: MRI and laser scanning.	Uterine cervix, LA, and sacrospinous ligaments.	Head and body. Articulated neck.	Isotropic nonlinear material. Neo-Hookean model.	Fetal head and fetal body: Nondeformable. Fetal neck: linear and rotational articulation.	Not imposed.

Note: BP—brachial plexus, OBI—obturator internus, TALA—tendinous arch of levator ani, LA—levator ani, VHP—visible human project.

Downloaded from http://asmedigitalcollection.asme.org/biomechanical/article-pdf/143/5/050801/6641401/bio_143_05_050801.pdf by Michigan State University user on 11 March 2021

multiple shorter incisions in terms of reducing the needed force to achieve delivery and protecting the pelvic musculature. However, it is worth pointing out that episiotomy itself is an invasive procedure. The above studies evaluated the effectiveness of episiotomy incision strategies strictly from a biomechanics perspective, without considering wound recovery postpartum. Therefore, conclusions like "the longer the episiotomy incision is, the lower the damage would be" need to be combined with the maternal prognosis following the incision wound in order to guide management during difficult labors. Many clinicians currently avoid any episiotomy unless additional room within the perineum is needed, as it has been shown that a laceration within the perineal tissues—and potentially into the pelvic tissues—will extend more easily from an initial episiotomy incision than from the undamaged skin.

During a shoulder dystocia event, obstetric maneuvers need to be adopted to facilitate the delivery and minimize the risk of overstretching the brachial plexus. Clinicians typically first resort to the McRoberts' maneuver and then suprapubic pressure. If the delivery does not proceed, clinicians will often use the posterior arm delivery maneuver or internal rotational maneuvers. With an earlier study showing the effectiveness of the McRoberts' maneuver [58], Grimm et al. [59] further investigated how suprapubic pressure, posterior arm delivery, and internal rotation would affect the delivery force and brachial plexus stretch using the same modeling framework, which included a fetal model with a fully articulated neck and shoulder. Lithotomy position (45 deg angle between the pubic symphysis and the horizontal plane) with clinician-applied traction on fetal head in the direction of 45 deg from the horizontal served as the baseline model. Suprapubic pressure was modeled as a vertically applied force on soft tissues above the maternal pubic symphysis. Three suprapubic pressure levels were simulated (40 N, 80 N, and 140 N). For oblique positioning, the fetus was rotated by 15 deg along its long axis from the baseline occipito-transverse position. The posterior arm delivery maneuver, as suggested by the name, had the posterior arm delivered before the simulation started. Results showed that all three maneuvers were effective in terms of reducing required delivery force and resulting brachial plexus stretch. Posterior arm delivery was associated with the lowest delivery force and greatest reduction in brachial plexus stretch. The delivery force and brachial plexus stretch of oblique positioning were comparable to those that resulted from higher level suprapubic pressure (40 N and 80 N). The increase in suprapubic pressure contributed to lower delivery forces and greater reduction of brachial plexus stretching. Similar to episiotomy simulations discussed above, these results from simulations of shoulder dystocia maneuvers are also strictly from a biomechanics perspective. The increased suprapubic pressure might be detrimental to the mother, and the action of delivering the posterior arm, which was not simulated in this study, could directly cause fetal injuries (e.g., humeral fracture) [74,75], even if performed correctly.

Thus, in all cases, the biomechanical knowledge gained from computational models should be combined with clinical judgment and experience when determining what approaches make sense for a particular delivery.

4 Summary

Childbirth computational modeling has come a long way in the last three decades and significantly advanced our knowledge of the mechanics and mechanical sequelae of childbirth. The characteristics of childbirth computational models discussed in this review paper have been summarized in Table 1. These models have provided useful insights for researchers into understand the mechanisms of birth-related injuries and for clinicians to scientifically evaluate ways to manage difficult labors in efficient and effective manners. However, there are still drawbacks to current studies that limit the comprehensive, biofidelic simulation of the childbirth process. As discussed in this review, the summary of childbirth computational models currently in the literature is as follows:

- The topics of the studies have focused on maternal injuries that result from childbirth, primarily on pelvic floor injuries. Therefore, the levator ani muscles are the most commonly represented maternal structures in these models, followed by perineal soft tissues.
- Fetal models have predominantly been head-only models—with some studies having a fetal trunk representation, but rarely with joint articulation.
- The delivery is generally driven by prescribed displacements or forces.
- The constitutive equations for the maternal soft tissues have begun to take viscoelasticity into consideration in recent studies. Transversely isotropic mechanical behavior has been widely adopted, while simpler isotropic hyperelastic models (i.e., neo-Hookean model and Mooney–Rivlin model) are still popular.
- Fetal models are usually described by rigid materials or elastic materials with very high stiffness.

To achieve more biofidelic childbirth simulation and explore broader childbirth related research questions using computational methods, the following efforts are still needed in future studies:

(1) *Develop a complete representation of the maternal soft tissues, including pelvic floor structures and pelvic organs*. A fundamental characteristic of childbirth is that the fetus is confined in a very limited space. Nonetheless, fetuses are mostly "floating" in open space above the maternal pelvis in existing models, due to the lack of maternal soft tissues. Despite the fact that geometrical models of maternal pelvic floor and pelvic organs have been developed in numerous studies [76–81], childbirth computational models rarely include structures other than levator ani muscles. This leads to inaccurate estimations of the resistive force that the fetal model experiences and requires an imposed trajectory and movements to obtain stable fetal passage through the pelvis. Critical physiological processes during childbirth, like uterine contractions and maternal pushing, cannot be fully simulated due to the lack of pelvic organ representation. In addition, the cardinal movements, which could lead to fetal malpositioning and potential fetal/maternal injuries, cannot be adequately and naturally produced in a simulation that lacks maternal soft tissues (e.g., uterus, cervix, vagina, bladder, rectum, and superficial perineal structures).

(2) *Develop a fetal model with full joint articulations and representation of fetal soft tissues*. Fetal joint articulations, especially fetal neck articulations, are crucial in producing the cardinal movements. The fetal shoulder joint structures are essential in assessing injuries like neonatal brachial plexus palsy. Fetal soft tissue representation could further advance the contact interaction accuracy during the fetal descent and help to achieve more precise estimates of delivery force and maternal soft tissue deformation.

(3) *Develop models with population-based generic data and adjustable parameters*. The ultimate goal of childbirth computational modeling is to predict labor outcomes and guide difficult labor management. Efficiency and accuracy are crucial to achieve this goal. Generic childbirth models need to be established to represent the population at different percentiles, based on anthropometric measurements that are easy to measure (e.g., height and weight). Measurements in the childbirth model that are critical to the delivery process (e.g., fetal head diameters, fetal shoulder width, and maternal pelvis measurements) should be made adjustable. Based on data obtained from clinical visits close to delivery, patient-specific childbirth models can be generated from corresponding generic models and may be able to improve our prediction of labor outcomes.

(4) *Develop models with patient-specific soft tissue properties*. Childbirth simulation studies have widely adopted patient-specific geometry for maternal soft tissues using MRI data.

Downloaded from http://asmedigitalcollection.asme.org/biomechanical/article-pdf/143/5/050801/6641401/bio_143_05_050801.pdf by Michigan State University user on 11 March 2021

However, the soft tissue mechanical properties are mostly based on animal tissues or human tissues from different individuals. The wide variation in soft tissue mechanical properties between species and even between individuals is the main reason that the predicted stress distribution patterns are currently of much more significance than the specific stress values provided through existing computational studies. Methods for in vivo soft tissue mechanical properties acquisition, such as magnetic resonance elastography [82] and ultrasonography [83], should be further explored and integrated into childbirth computational modeling. Until then, increasing the library of human tissue properties—preferably for tissues from gravid women—will allow for improved parametric modeling to be conducted.

(5) *Develop improved methods for model validation*. Along with the improvements mentioned above, options for the validation of childbirth models also need significant improvement. With real-time imaging techniques like live MRI, patient-specific real-time in vivo data (e.g., pelvic floor soft tissue deformation, and the cardinal movements of the fetus) could be used to validate both patient-specific and general computational models. This comparison between in vivo and computational data can also help to tune certain parameters that are difficult to measure (e.g., the friction coefficient between the fetus and maternal soft tissues). To date, the authors are not aware of any attempts in the literature to use primary validation (i.e., comparing actual output predictions to experimentally measured data) for models of childbirth. Secondary validation (e.g., comparing delivery forces and the motion of the infant [58,59]) has been utilized to confirm that predictions from models are reasonable.

Computational models of childbirth are an important tool to better understand a process—including interventions and possible injurious outcomes—that cannot easily or ethically be studied in a clinical setting. The models that have been developed over the past 30 years have added significantly to our understanding of this truly biomechanical process. The increased number of researchers who are interested in reproductive biomechanics, as well as the recent advancements in the computational techniques used in childbirth models, makes us optimistic that the questions that we are asking now are just the beginning—and that such computational models will continue to inform and advance clinical practice in obstetrics in the coming years.

Funding Data

- National Science Foundation (Grant No. NSF 2028474 (CBET—DARE); Funder ID: 10.13039/100000001).

References

[1] Grimm, M. J., 2016, "Maternal Endogenous Forces and Shoulder Dystocia," Clin. Obstet. Gynecol., **59**(4), pp. 820–829.

[2] Chaliha, C., 2009, "Postpartum Pelvic Floor Trauma," Curr. Opin. Obstet. Gynecol., **21**(6), pp. 474–479.

[3] American College of Obstetricians and Gynecologists 2014, *Neonatal Brachial Plexus Palsy*, The American College of Obstetricians and Gynecologists, Women's Health Care Physicians, Washington, DC.

[4] Crofts, J. F., Attilakos, G., Read, M., Sibanda, T., and Draycott, T. J., 2005, "Shoulder Dystocia Training Using a New Birth Training Mannequin," BJOG: Int. J. Obstet. Gynaecol., **112**(7), pp. 997–999.

[5] Crofts, J. F., Bartlett, C., Ellis, D., Hunt, L. P., Fox, R., and Draycott, T. J., 2007, "Management of Shoulder Dystocia: Skill Retention 6 and 12 Months After Training," Obstet. Gynecol., **110**(5), pp. 1069–1074.

[6] Moreau, R., Ochoa, V., Pham, M. T., Boulanger, P., Redarce, T., and Dupuis, O., 2007, "Evaluation of Obstetric Gestures: An Approach Based on the Curvature of 3-D Positions," 29th Annual International Conference of the IEEE Engineering in Medicine and Biology Society, Lyon, France, Aug. 23–26, pp. 3634–3637.

[7] Gurewitsch, E. D., Kim, E. J., Yang, J. H., Outland, K. E., McDonald, M. K., and Allen, R. H., 2005, "Comparing McRoberts' and Rubin's Maneuvers for Initial Management of Shoulder Dystocia: An Objective Evaluation," Am. J. Obstet. Gynecol., **192**(1), pp. 153–160.

[8] Kim, E. J., Theprungsirikul, P., McDonald, M. K., Gurewithsch, E. D., and Allen, R. H., 2005, "A Biofidelic Birthing Simulator," IEEE Eng. Med. Biol. Mag., **24**(6), pp. 34–39.

[9] Allen, R. H., Cha, S. L., Kranker, L. M., Johnson, T. L., and Gurewitsch, E. D., 2007, "Comparing Mechanical Fetal Response During Descent, Crowning, and Restitution Among Deliveries With and Without Shoulder Dystocia," Am. J. Obstet. Gynecol., **196**(6), p. 539.

[10] Lehn, A. M., Baumer, A., and Leftwich, M. C., 2016, "An Experimental Approach to a Simplified Model of Human Birth," J. Biomech., **49**(11), pp. 2313–2317.

[11] Noritomi, P. Y., da Silva, J. V. L., Dellai, R. C. A., Fiorentino, A., Giorleo, L., and Ceretti, E., 2013, "Virtual Modeling of a Female Pelvic Floor and Hypothesis for Simulating Biomechanical Behavior During Natural Delivery," Procedia CIRP, **5**, pp. 300–304.

[12] Berardi, M., Martinez-Romero, O., Elías-Zúñiga, A., Rodríguez, M., Ceretti, E., Fiorentino, A., Donzella, G., and Avanzini, A., 2014, "Levator Ani Deformation During the Second Stage of Labour," Proc. Inst. Mech. Eng. H, **228**(5), pp. 501–508.

[13] Li, X., Kruger, J. A., Chung, J.-H., Nash, M. P., and Nielsen, P. M. F., 2008, "Modelling Childbirth: Comparing Athlete and Non-Athlete Pelvic Floor Mechanics," Medical Image Computing and Computer-Assisted Intervention—MICCAI 2008, D. Metaxas, L. Axel, G. Fichtinger, and G. Székely, eds., Springer, Berlin, Heidelberg, pp. 750–757.

[14] Li, X., Kruger, J. A., Nash, M. P., and Nielsen, P. M. F., 2010, "Effects of Fetal Head Motion on Pelvic Floor Mechanics," Computational Biomechanics for Medicine, K. Miller, and P. M. F. Nielsen, eds., Springer, New York, pp. 129–137.

[15] Liu, Y., Scudder, M., and Gimovsky, M. L., 1996, "CAD Modeling of the Birth Process. Part II," Stud. Health Technol. Inform., **29**, pp. 652–666.

[16] Yan, X., Kruger, J. A., Nielsen, P. M. F., and Nash, M. P., 2015, "Effects of Fetal Head Shape Variation on the Second Stage of Labour," J. Biomech., **48**(9), pp. 1593–1599.

[17] Lien, K.-C., Mooney, B., DeLancey, J. O. L., and Ashton-Miller, J. A., 2004, "Levator Ani Muscle Stretch Induced by Simulated Vaginal Birth," Obstet. Gynecol., **103**(1), pp. 31–40.

[18] Lien, K.-C., Morgan, D. M., Delancey, J. O. L., and Ashton-Miller, J. A., 2005, "Pudendal Nerve Stretch During Vaginal Birth: A 3D Computer Simulation," Am. J. Obstet. Gynecol., **192**(5), pp. 1669–1676.

[19] Hoyte, L., Damaser, M. S., Warfield, S. K., Chukkapalli, G., Majumdar, A., Choi, D. J., Trivedi, A., and Krysl, P., 2008, "Quantity and Distribution of Levator Ani Stretch During Simulated Vaginal Childbirth," Am. J. Obstet. Gynecol., **199**(2), p. 198.

[20] Buttin, R., Zara, F., Shariat, B., and Redarce, T., 2009, "A Biomechanical Model of the Female Reproductive System and the Fetus for the Realization of a Childbirth Virtual Simulator," Annual International Conference of the IEEE Engineering in Medicine and Biology Society, Minneapolis, MN, Sept. 2–6, pp. 5263–5266.

[21] Li, X., Kruger, J. A., Nash, M. P., and Nielsen, P. M. F., 2011, "Anisotropic Effects of the Levator Ani Muscle During Childbirth," Biomech. Model Mechanobiol., **10**(4), pp. 485–494.

[22] Buttin, R., Zara, F., Shariat, B., Redarce, T., and Grangé, G., 2013, "Biomechanical Simulation of the Fetal Descent Without Imposed Theoretical Trajectory," Comput. Methods Prog. Biomed., **111**(2), pp. 389–401.

[23] Gerikhanov, Z., Audinis, V., and Lapeer, R., 2013, "Towards a Forward Engineered Simulation of the Cardinal Movements of Human Childbirth," E-Health and Bioengineering Conference (EHB), Iasi, Romania, Nov. 21–23, pp. 1–4.

[24] Lepage, J., Jayyosi, C., Lecomte-Grosbras, P., Brieu, M., Duriez, C., Cosson, M., and Rubod, C., 2015, "Biomechanical Pregnant Pelvic System Model and Numerical Simulation of Childbirth: Impact of Delivery on the Uterosacral Ligaments, Preliminary Results," Int. Urogynecol. J., **26**(4), pp. 497–504.

[25] Krofta, L., Havelková, L., Urbánková, I., Krčmář, M., Hynčík, L., and Feyereisl, J., 2017, "Finite Element Model Focused on Stress Distribution in the Levator Ani Muscle During Vaginal Delivery," Int. Urogynecol. J., **28**(2), pp. 275–284.

[26] Mayeur, O., Jeanditgautier, E., Witz, J.-F., Lecomte-Grosbras, P., Cosson, M., Rubod, C., and Brieu, M., 2017, "Evaluation of Strains on Levator Ani Muscle: Damage Induced During Delivery for a Prediction of Patient Risks," Computational Biomechanics for Medicine, A. Wittek, G. Joldes, P. M. F. Nielsen, B. J. Doyle, and K. Miller, eds., Springer International Publishing, Cham, pp. 135–146.

[27] Maran, J.-C., Cassagnes, L., Delmas, V., Musset, D., Frydman, R., Mage, G., Canis, M., Boyer, L., and Ami, O., 2018, "Comparative Anatomy on 3-D MRI of the Urogenital Sinus and the Periurethral Area Before and During the Second Stage of Labor During Childbirth," Surg. Radiol. Anat., **40**(4), pp. 371–380.

[28] Jean Dit Gautier, E., Mayeur, O., Lepage, J., Brieu, M., Cosson, M., and Rubod, C., 2018, "Pregnancy Impact on Uterosacral Ligament and Pelvic Muscles Using a 3D Numerical and Finite Element Model: Preliminary Results," Int. Urogynecol. J., **29**(3), pp. 425–430.

[29] Silva, M. E. T., Oliveira, D. A., Roza, T. H., Brandão, S., Parente, M. P. L., Mascarenhas, T., and Natal Jorge, R. M., 2015, "Study on the Influence of the Fetus Head Molding on the Biomechanical Behavior of the Pelvic Floor Muscles, During Vaginal Delivery," J. Biomech., **48**(9), pp. 1600–1605.

[30] Liu, Y., Scudder, M., and Gimovsky, M. L., 1995, "CAD Modelling of the Birth Process: A Preliminary Report," Proceedings of Medicine Meets Virtual Reality Conference III: Interactive Technology & the New Paradigm for Healthcare, San Diego, CA, Jan 19–22, pp. 211–220.

[31] Sindhwani, N., Bamberg, C., Famaey, N., Callewaert, G., Dudenhausen, J. W., Teichgräber, U., and Deprest, J., 2017, "In Vivo Evidence of Significant Levator Ani Muscle Stretch on MR Images of a Live Childbirth," Am. J. Obstet. Gynecol., **217**(2), p. 194.

[32] Bamberg, C., Deprest, J., Sindhwani, N., Teichgräberg, U., Güttler, F., Dudenhausen, J. W., Kalache, K. D., and Henrich, W., 2017, "Evaluating Fetal Head

Downloaded from http://asmedigitalcollection.asme.org/biomechanical/article-pdf/143/5/050801/6641401/bio_143_05_050801.pdf by Michigan State University user on 11 March 2021

Dimension Changes During Labor Using Open Magnetic Resonance Imaging," J. Perinatal Med., **45**(3), pp. 305–308.
[33] Janda, Š., van der Helm, F. C. T., and de Blok, S. B., 2003, "Measuring Morphological Parameters of the Pelvic Floor for Finite Element Modelling Purposes," J. Biomech., **36**(6), pp. 749–757.
[34] Martins, J. A. C., Pato, M. P. M., Pires, E. B., Jorge, R. M. N., Parente, M., and Mascarenhas, T., 2007, "Finite Element Studies of the Deformation of the Pelvic Floor," Ann. New York Acad. Sci., **1101**(1), pp. 316–334.
[35] Parente, M. P. L., Jorge, R. M. N., Mascarenhas, T., Fernandes, A. A., and Martins, J. A. C., 2007, "Deformation of the Pelvic Floor Muscles During a Vaginal Delivery," Int. Urogynecol. J., **19**(1), pp. 65–71.
[36] Oliveira, D. A., Parente, M. P. L., Calvo, B., Mascarenhas, T., and Natal Jorge, R. M., 2016, "Numerical Simulation of the Damage Evolution in the Pelvic Floor Muscles During Childbirth," J. Biomech., **49**(4), pp. 594–601.
[37] Parente, M. P., Natal Jorge, R. M., Mascarenhas, T., and Silva-Filho, A. L., 2010, "The Influence of Pelvic Muscle Activation During Vaginal Delivery," Obstet. Gynecol., **115**(4), pp. 804–808.
[38] Parente, M. P. L., Jorge, R. M. N., Mascarenhas, T., Fernandes, A. A., and Martins, J. A. C., 2009, "The Influence of an Occipito-Posterior Malposition on the Biomechanical Behavior of the Pelvic Floor," Eur. J. Obstet. Gynecol. Reproduct. Biol., **144**, pp. S166–S169.
[39] Oliveira, D. A., Parente, M. P. L., Calvo, B., Mascarenhas, T., and Jorge, R. M. N., 2016, "A Biomechanical Analysis on the Impact of Episiotomy During Childbirth," Biomech. Model Mechanobiol., **15**(6), pp. 1523–1534.
[40] Oliveira, D. A., Parente, M. P. L., Calvo, B., Mascarenhas, T., and Jorge, R. M. N., 2017, "The Management of Episiotomy Technique and Its Effect on Pelvic Floor Muscles During a Malposition Childbirth," Comput. Methods Biomech. Biomed. Eng., **20**(11), pp. 1249–1259.
[41] d'Aulignac, D., Martins, J. A. C., Pires, E. B., Mascarenhas, T., and Jorge, R. M. N., 2005, "A Shell Finite Element Model of the Pelvic Floor Muscles," Comput. Methods Biomech. Biomed. Eng., **8**(5), pp. 339–347.
[42] Parente, M. P., Natal Jorge, R. M., Mascarenhas, T., Fernandes, A. A., and Silva-Filho, A. L., 2010, "Computational Modeling Approach to Study the Effects of Fetal Head Flexion During Vaginal Delivery," Am. J. Obstet. Gynecol., **203**(3), p. 217.
[43] Vila Pouca, M. C. P., Ferreira, J. P. S., Oliveira, D. A., Parente, M. P. L., Mascarenhas, T., and Natal Jorge, R. M., 2018, "On the Effect of Labour Durations Using an Anisotropic Visco-Hyperelastic-Damage Approach to Simulate Vaginal Deliveries," J. Mech. Behav. Biomed. Mater., **88**, pp. 120–126.
[44] Pouca, M. C. P. V., Ferreira, J. P. S., Oliveira, D. A., Parente, M. P. L., and Jorge, R. M. N., 2018, "Viscous Effects in Pelvic Floor Muscles During Childbirth: A Numerical Study," Int. J. Numer. Methods Biomed. Eng., **34**(3), p. e2927.
[45] Lapeer, R., Gerikhanov, Z., Sadulaev, S.-M., Audinis, V., Rowland, R., Crozier, K., and Morris, E., 2019, "A Computer-Based Simulation of Childbirth Using the Partial Dirichlet–Neumann Contact Method With Total Lagrangian Explicit Dynamics on the GPU," Biomech. Model Mechanobiol., **18**(3), pp. 681–700.
[46] Routzong, M. R., Moalli, P. A., Maiti, S., De Vita, R., and Abramowitch, S. D., 2019, "Novel Simulations to Determine the Impact of Superficial Perineal Structures on Vaginal Delivery," Interface Focus, **9**(4), p. 20190011.
[47] Lapeer, R., Audinis, V., Gerikhanov, Z., and Dupuis, O., 2014, "A Computer-Based Simulation of Obstetric Forceps Placement," Medical Image Computing and Computer-Assisted Intervention—MICCAI 2014, P. Golland, N. Hata, C. Barillot, J. Hornegger, and R. Howe, eds., Springer International Publishing, Cham, pp. 57–64.
[48] Bailet, M., Zara, F., and Promayon, E., 2014, "Biomechanical Model of the Fetal Head for Interactive Childbirth Simulation," SURGETICA 2014 Computer-Assisted Medical Interventions: Scientific Problems, Tools and Clinical Applications, Chambéry, France, pp. 116–119, HAL No. hal-01301093.
[49] Oliveira, D., Pouca, M. V., Ferreira, J., and Mascarenhas, T., 2019, "Episiotomy: The Biomechanical Impact of Multiple Small Incisions During a Normal Vaginal Delivery," Interface Focus, **9**(5), p. 20190027.
[50] Bailet, M., Zara, F., and Promayon, E., 2013, "Shell Finite Element Model for Interactive Foetal Head Deformation During Childbirth," Comput. Methods Biomech. Biomed. Eng., **16**(sup1), pp. 312–314.
[51] Li, X., Kruger, J. A., Chung, J.-H., Nash, M. P., and Nielsen, P. M. F., 2008, "Modelling the Pelvic Floor for Investigating Difficulties During Childbirth," Proc. SPIE 6916, Medical Imaging 2008: Physiology, Function, and Structure From Medical Images, San Diego, CA, Mar. 12, p. 69160V.
[52] Li, X., Kruger, J. A., Nash, M. P., and Nielsen, P. M. F., 2010, "Effects of Nonlinear Muscle Elasticity on Pelvic Floor Mechanics During Vaginal Childbirth," ASME J. Biomech. Eng., **132**(11), p. 111010.
[53] Yan, X., Kruger, J. A., Nash, M. P., and Nielsen, P. M. F., 2012, "Effects of Levator Ani Muscle Morphology on the Mechanics of Vaginal Childbirth," Computational Biomechanics for Medicine, P. M. F. Nielsen, A. Wittek, and K. Miller, eds., Springer, New York, pp. 63–75.
[54] Oliveira, D., Parente, M., Mascarenhas, T., and Natal Jorge, R., 2018, "Biomechanical Analysis of the Damage in the Pelvic Floor Muscles During Childbirth," Women's Health and Biomechanics: Where Medicine and Engineering Meet, S. Brandão, T. Da Roza, I. Ramos, and T. Mascarenhas, eds., Springer International Publishing, Cham, pp. 133–142.
[55] Vila Pouca, M. C. P., Ferreira, J. P. S., Oliveira, D. A., Parente, M. P. L., Mascarenhas, M. T., and Natal Jorge, R. M., 2019, "Simulation of the Uterine Contractions and Foetus Expulsion Using a Chemo-Mechanical Constitutive Model," Biomech. Model Mechanobiol., **18**(3), pp. 829–843.
[56] Oliveira, D. A., Silva, M. E. T., Pouca, M. V., Parente, M. P. L., Mascarenhas, T., and Natal Jorge, R. M., 2020, "Biomechanical Simulation of Vaginal Childbirth: The Colors of the Pelvic Floor Muscles," Computational Biomechanics for Medicine, M. P. Nash, P. M. F. Nielsen, A. Wittek, K. Miller, and G. R. Joldes, eds., Springer International Publishing, Cham, pp. 1–17.
[57] Gonik, B., Zhang, N., and Grimm, M. J., 2003, "Defining Forces That Are Associated With Shoulder Dystocia: The Use of a Mathematic Dynamic Computer Model," Am. J. Obstet. Gynecol., **188**(4), pp. 1068–1072.
[58] Gonik, B., Zhang, N., and Grimm, M. J., 2003, "Prediction of Brachial Plexus Stretching During Shoulder Dystocia Using a Computer Simulation Model," Am. J. Obstet. Gynecol., **189**(4), pp. 1168–1172.
[59] Grimm, M. J., Costello, R. E., and Gonik, B., 2010, "Effect of Clinician-Applied Maneuvers on Brachial Plexus Stretch During a Shoulder Dystocia Event: Investigation Using a Computer Simulation Model," Am. J. Obstet. Gynecol., **203**(4), p. 339.
[60] Lapeer, R., Gerikhanov, Z., and Audinis, V., 2014, "A Computer-Based Simulation of Vacuum Extraction During Childbirth," SIMULIA Regional User Meeting RUM, Warrington, UK, Nov. 4–5, pp. 1–12.
[61] Li, X., Kruger, J., Nash, M., and Nielsen, P., 2009, "Modelling Fetal Head Motion and Its Mechanical Interaction With the Pelvic Floor During Childbirth," 39th International Meeting of the International Continence Society, Wiley-Liss, San Francisco, CA, Sept. 29–Oct. 3, p. 81.
[62] Pintar, F. A., Mayer, R. G., Yoganandan, N., and Sun, E., 2000, "Child Neck Strength Characteristics Using an Animal Model," Stapp Car Crash J., **44**, pp. 77–83.
[63] Rydevik, B. L., Kwan, M. K., Myers, R. R., Brown, R. A., Triggs, K. J., Woo, S. L.-Y., and Garfin, S. R., 1990, "An In Vitro Mechanical and Histological Study of Acute Stretching on Rabbit Tibial Nerve," J. Orthop. Res., **8**(5), pp. 694–701.
[64] Jansova, M., Kalis, V., Rusavy, Z., Zemcik, R., Lobovsky, L., and Laine, K., 2014, "Modeling Manual Perineal Protection During Vaginal Delivery," Int. Urogynecol. J., **25**(1), pp. 65–71.
[65] Jansova, M., Kalis, V., Rusavy, Z., Räisänen, S., Lobovsky, L., and Laine, K., 2017, "Fetal Head Size and Effect of Manual Perineal Protection," PLoS One, **12**(12), p. e0189842.
[66] Sorbe, B., and Dahlgren, S., 1983, "Some Important Factors in the Molding of the Fetal Head During Vaginal Delivery—A Photographic Study," Int. J. Gynecol. Obstet., **21**(3), pp. 205–212.
[67] Lapeer, R. J., and Prager, R. W., 2001, "Fetal Head Moulding: Finite Element Analysis of a Fetal Skull Subjected to Uterine Pressures During the First Stage of Labour," J. Biomech., **34**(9), pp. 1125–1133.
[68] Sizer, A. R., and Nirmal, D. M., 2000, "Occipitoposterior Position: Associated Factors and Obstetric Outcome in Nulliparas," Obstet. Gynecol., **96**(5, Part 1), pp. 749–752.
[69] Hage-Fransen, M. A. H., Wiezer, M., Otto, A., Wieffer-Platvoet, M. S., Slotman, M. H., Sanden, M. W. G. N. der, and Pool-Goudzwaard, A. L., 2020, "Pregnancy- and Obstetric-Related Risk Factors for Urinary Incontinence, Fecal Incontinence, or Pelvic Organ Prolapse Later in Life: A Systematic Review and Meta-Analysis," Acta Obstet. Gynecol. Scand., ePub.
[70] Su, K.-M., Yu, M.-H., Su, H.-Y., Wang, Y.-C., and Su, K.-C., 2016, "Investigating Biomechanics of Different Materials and Angles of Blades of Forceps for Operative Delivery by Finite Element Analysis," J. Mech. Med. Biol., **16**(04), p. 1650046.
[71] Doumouchtsis, S. K., and Arulkumaran, S., 2008, "Head Trauma After Instrumental Births," Clin. Perinatol., **35**(1), pp. 69–83.
[72] Edozien, L. C., 2007, "Towards Safe Practice in Instrumental Vaginal Delivery," Best Pract. Res. Clin. Obstet. Gynaecol., **21**(4), pp. 639–655.
[73] Barnes, R. S. F., 1883, *A Manual of Midwifery for Midwives*, Smith, Elder, & Co., London, UK.
[74] Menticoglou, S., 2018, "Shoulder Dystocia: Incidence, Mechanisms, and Management Strategies," Int J Womens Health, **10**, pp. 723–732.
[75] Gherman, R. B., Ouzounian, J. G., and Goodwin, T. M., 1998, "Obstetric Maneuvers for Shoulder Dystocia and Associated Fetal Morbidity," Am. J. Obstet. Gynecol., **178**(6), pp. 1126–1130.
[76] Ren, S., Xie, B., Wang, J., and Rong, Q., 2015, "Three-Dimensional Modeling of the Pelvic Floor Support Systems of Subjects With and Without Pelvic Organ Prolapse," Biomed. Res. Int., **2015**, pp. 1–9.
[77] Giraudet, G., Patrouix, L., Fontaine, C., Demondion, X., Cosson, M., and Rubod, C., 2018, "Three Dimensional Model of the Female Perineum and Pelvic Floor Muscles," Eur. J. Obstet. Gynecol. Reprod. Biol., **226**, pp. 1–6.
[78] Feil, P., and Sora, M., 2014, "A 3D Reconstruction Model of the Female Pelvic Floor by Using Plastinated Cross Sections," Austin J. Anat., **1**(5), p. 1022.
[79] Gatellier, M.-A., dit Gautier, E. J., Mayeur, O., Brieu, M., Cosson, M., and Rubod, C., 2020, "Complete 3 Dimensional Reconstruction of Parturient Pelvic Floor," J. Gynecol. Obstet. Human Reprod., **49**(1), p. 101635.
[80] Wu, Y., Hikspoors, J. P. J. M., Mommen, G., Dabhoiwala, N. F., Hu, X., Tan, L.-W., Zhang, S.-X., and Lamers, W. H., 2020, "Interactive Three-Dimensional Teaching Models of the Female and Male Pelvic Floor," Clin. Anat., **33**(2), pp. 275–285.
[81] Brandão, F. S. Q., da, S., Parente, M. P. L., Rocha, P. A. G. G., Saraiva, M. T., da, Q. e C., de, M., Ramos, I. M. A. P., and Jorge, R. M. N., 2016, "Modeling the Contraction of the Pelvic Floor Muscles," Comput. Methods Biomech. Biomed. Eng., **19**(4), pp. 347–356.
[82] Hiscox, L. V., Johnson, C. L., Barnhill, E., McGarry, M. D. J., Huston, J., Beek, E. J. R. van, Starr, J. M., and Roberts, N., 2016, "Magnetic Resonance Elastography (MRE) of the Human Brain: Technique, Findings and Clinical Applications," Phys. Med. Biol., **61**(24), pp. R401–R437.
[83] Dargar, S., Akyildiz, A. C., and De, S., 2017, "In Situ Mechanical Characterization of Multilayer Soft Tissue Using Ultrasound Imaging," IEEE Trans. Biomed. Eng., **64**(11), pp. 2595–2606.

Downloaded from http://asmedigitalcollection.asme.org/biomechanical/article-pdf/143/5/050801/6641401/bio_143_05_050801.pdf by Michigan State University user on 11 March 2021